Polymer Chemistry

Reversible Cyclic-Linear Topological Transformation using a Long-Range Rotaxane Switch

Journal:	*Polymer Chemistry*
Manuscript ID	PY-COM-09-2021-001197.R1
Article Type:	Communication
Date Submitted by the Author:	06-Oct-2021
Complete List of Authors:	Aoki, Daisuke; Tokyo Institute of Technology, Chemical Science and Engineering Aibara, Gota ; Tokyo Institute of Technology Takata, Toshikazu; Tokyo Institute of Technology, Materials and Chemical Technology, Tokyo Institute of Technology; JST, Core Research for Evolutional Science and Technology

COMMUNICATION

Reversible Cyclic-Linear Topological Transformation using a Long-Range Rotaxane Switch

Daisuke Aoki,[a] Gota Aibara,[a] and Toshikazu Takata*[a,b,c]

Received 00th January 20xx,
Accepted 00th January 20xx

DOI: 10.1039/x0xx00000x

A reversible linear-cyclic topological transformation of a poly(ε-caprolactone) facilitated by a long-range rotaxane switch is reported. A linear polymer, whose topology is fixed by a protonated *tert*-amine/crown ether interaction at the center of the polymer chain, was reversibly transformed into a cyclic polymer fixed by urethane linkage/crown ether interaction at the polymer end upon neutralization/acidification of the *tert*-amine moiety.

Thanks to the recent progress in polymer chemistry, various topological polymers (e.g., star, hyperbranched, and cyclic polymers) have been synthesized and characterized.[1-10] As the topology effect in polymers has been observed not only in solution but also in the bulk state, topological transformations in polymers have been identified as a novel tool to change their macroscopic properties. Among these topological transformations, reversible ones would be ideal to build novel types of stimuli-responsive polymers that can respond to a broad range of stimuli.[11] However, such reversible transformations of polymer chains are challenging, especially without changing the molecular weight and/or composition of the polymer. To achieve reversible topological transformations in polymers, various dynamic linkages such as multipoint-hydrogen bonds[12], metal-coordination bonds[13], host-guest interactions[14], and dynamic covalent bonds[15, 16] have been investigated, and these can change the polymer topology by association/dissociation of the dynamic linkage. As the association/dissociation reactions of dynamic linkages are carried out under conditions of equilibrium control, linear-cyclic transformations usually occur under dilute conditions, while cyclic-linear transformations often proceed under concentrated conditions. For example, Yamamoto *et al.* successfully demonstrated a reversible linear-cyclic topological transformation via photodimerization of the anthryl group at the end of a polymer chain.[17] Association/dissociation of the anthracene group triggered by light or heat enabled a reversible linear-cyclic topological transformation. Although these unique reversible transformations showcase the potential toward further applications as novel stimuli-responsive materials, examples remain scarce. It should be noted here that most topological transformations that proceed without change in molecular weight and/or composition, require concentration control to induce a selective transformation, thus limiting their trigger conditions and applications as high-performance materials based on the change in polymer topology.

Recently, we have developed a polymer-topological-transformation system based on a long-range rotaxane protocol in which the wheel position can be controlled by changing the interaction with the polymeric axle chain.[18, 19] In comparison with conventional dynamic systems that use a dynamic linkage, rotaxane-based topology transformations do not require highly diluted conditions or elaborate reaction and purification protocols. Based on this long-range rotaxane strategy, we have accomplished star-linear[20, 21] and linear-cyclic[22-26] topological transformations. Especially, linear-cyclic topological transformations facilitated by a [c2]-daisy-chain structure can be used as an effective method for the large-scale synthesis of cyclic polymers given that the cyclization process is automatic, quantitative, and concentration-independent via the self-assembly of *sec*-ammonium-containing crown ethers to afford [c2] daisy chains as small circles, which are subsequently expanded to cyclic polymers via the introduction of polymer chains followed by a linear-cyclic topological transformation (Figure 1a).[22] To further improve the utility of our system, we have investigated in this study a reversible cyclic-linear transformation based on a two-station-type rotaxane, in which a crown ether interacts with a *tert*-amine moiety at the α-end and a urethan linkage at the ω-end, that was applied to convert and fix the polymer topology. The interaction between the axle (polymer chain) and the wheel (crown ether) components can

[a] *Department of Chemical Science and Engineering, Tokyo Institute of Technology, Ookayama, Meguro, Tokyo 152-8552, Japan*
[b] *JST-CREST*
[c] *Graduate School of Advanced Science and Engineering, Hiroshima University, Kagamiyama, Higashi-Hiroshima, Hiroshima 739-8527, Japan*
Electronic Supplementary Information (ESI) available: [details of any supplementary information available should be included here]. See DOI: 10.1039/x0xx00000x

be switched by simple acidification/neutralization of the *tert*-amine moiety on the polymer chain (Figure 1b).

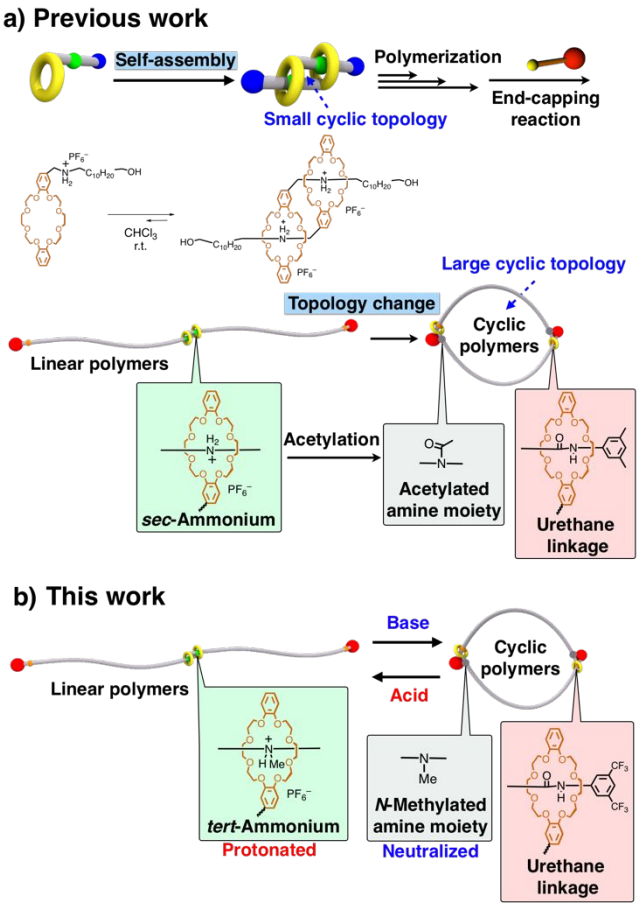

Figure 1. a) Synthetic route to cyclic polymers via the self-assembly of *sec*-ammonium-containing crown ethers to afford [c2] daisy chains (small circles), followed by introduction of polymer chains and a linear-cyclic topology transformation. b) Reversible linear-cyclic transformation based on a rotaxane switch upon neutralization/acidification of the *tert*-amine moiety.

Firstly, we synthesized linear poly(ε-caprolactone) (PCL) with a [c2] daisy chain at the center of the polymer chain (**PCL_S**; the suffix "S" indicates that the wheel component is fixed on the *sec*-ammonium moiety) by living ring-opening polymerization (ROP) of ε-caprolactone (CL) from a bifunctional initiator with a [c2] daisy chain (rotaxane dimer **1**) and *sec*-ammonium/crown ether interactions, followed by end-capping with a bulky isocyanate (Scheme 1). Accordingly, **1** was used as the initiator in the presence of diphenyl phosphate (DPP), resulting in the living ROP of CL using a $[CL]_0$ / $[\mathbf{1}]_0$ / $[DPP]_0$ ratio of 50/1.0/0.5 (CH_2Cl_2, 6 h, 10 °C). The polymerization was quenched by the addition of 3,5-bis(trifluoromethyl)phenyl isocyanate to cap the propagation end with a bulky stopper and to introduce a urethane moiety, which acts as a second recognition site at the end of the polymer chain. The thus obtained polymer was isolated by twofold reprecipitation from CH_2Cl_2 solution into ethanol/hexane (1/9, v/v), followed by reprecipitation from CH_2Cl_2 solution into hexane to obtain **PCL_S** (84%) as a white solid. The degree of polymerization was estimated by ^{1}H NMR spectroscopy (DP = 28, n = 14 in Scheme 1, $M_{n\ NMR}$ = 5320 Da).

Subsequently, the *sec*-ammonium moiety at the center of **PCL_S** was *N*-methylated to release the strong interaction between the *sec*-ammonium moiety and the crown ether wheel, which results in a linear topology. Namely, *N*-methylation[27-29] using paraformaldehyde and $NaBH(OAc)_3$ as the reducing agent in the presence of triethylamine was applied, which furnished **PCL_U** (the suffix "U" indicates that the wheel component is fixed on the urethane linkage). The thus obtained **PCL_U** was isolated by reprecipitation from NMP into water, followed by drying (61%). The structure of **PCL_U** was confirmed by MALDI-TOF mass spectrometry (Figure 2) and NMR spectroscopy (Figure 3a). Figure 2 shows the MALDI-TOF mass spectrum of **PCL_U**. The intervals between peaks (114 Da) correspond to the molecular weight of CL and coincides with the theorical value, thus confirming the successful synthesis of **PCL_U**.

Scheme 1. Synthesis of cyclic polymer **PCL_U** using a two-station-type rotaxane.

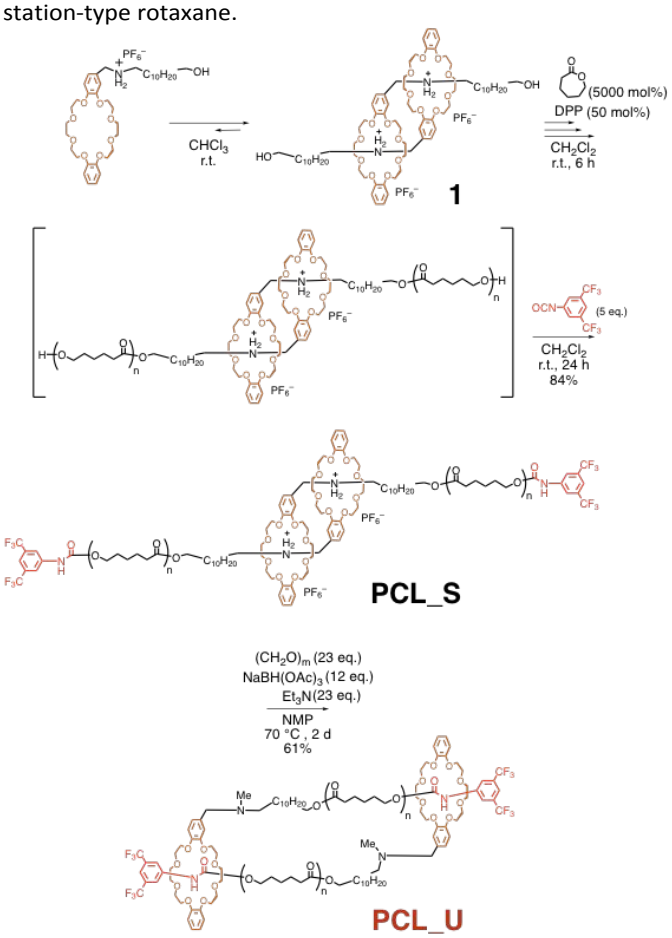

Then, we examined the acidification/neutralization-based shuttling behavior of **PCL_U** (Scheme 2). Protonation of the *tert*-amine moiety in **PCL_U** was accomplished using ammonium hexafluorophosphate, which afforded the linear polymer **PCL_T** (the suffix "T" indicates that the wheel component is fixed on the *tert*-ammonium moiety) supported by the [c2]-daisy-chain

structure wherein the *tert*-ammonium/crown ether interaction provides the linear topology. As the *N*-methylation facilitates the neutralization of the ammonium rotaxane, simple treatment with aqueous sodium carbonate restored **PCL_U**, wherein the urethane/crown ether interaction fixes the cyclic structure.

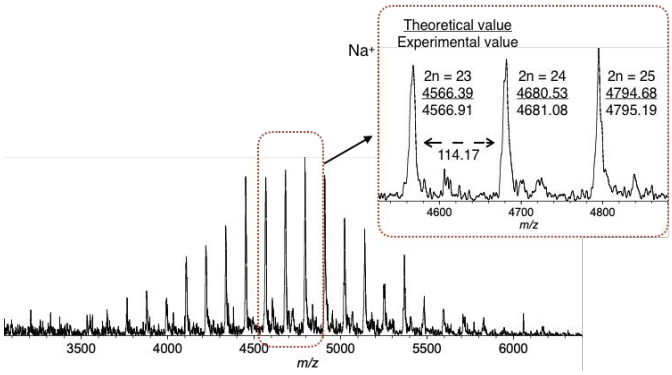

Figure 2. MALDI-TOF mass spectrum for **PCL_U**.

Scheme 2. Topological transformation by changing interactions between the urethane linkage/crown ether and the *tert*-ammonium/crown ether upon neutralization/acidification of the *tert*-amine moiety.

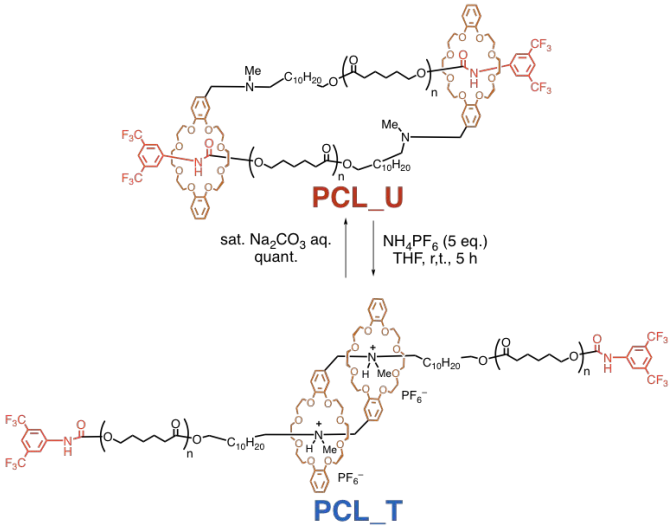

The location of the wheel component upon acidification/neutralization-based switching was confirmed by ^{1}H NMR spectroscopy. Figure 3 shows the ^{1}H NMR spectra of **PCL_U**, **PCL_T** (after protonation), and **PCL_U$_2$** (after neutralization; the subscript number denotes the number of neutralization/acidification processes). After protonation (Figure 3a vs 3b), the methylene peak adjacent to the *tert*-amine moiety that appeared at ~2.3 ppm (marked as *a*) in **PCL_U**, was shifted to 4.6 and 4.8 ppm (**PCL-T** in Figure 3b); moreover, the methyl signal of the amine (marked as *Me*) shifted from 2.1 ppm to 3.2 ppm, demonstrating that the crown ether is located on the protonated *tert*-amine moiety. In association with the movement of the crown ether, the peaks at the end of the polymer chain, i.e., the aromatic signals (especially peak *g*) and the active proton at the urethane linkage (marked as *e*), were also shifted. The corresponding ^{19}F NMR spectra further supported interactions between the crown ether and the urethane linkage (Figure S4).[24] When the crown ether was located on the urethane linkage, most of the peaks shifted to lower magnetic field, which is consistent with our previous reports. This peak shift is derived from the end-capped structure that supports the crown ether/urethane linkage interaction, which is the driving force to provide the cyclic structure. After neutralization (Figure 3b vs 3c), the peak positions returned and the spectrum was identical to that of **PCL_U**, demonstrating fully reversible positional changes of the crown ether via the acidification/neutralization-based rotaxane switch using the *tert*-amine moiety on the axle.

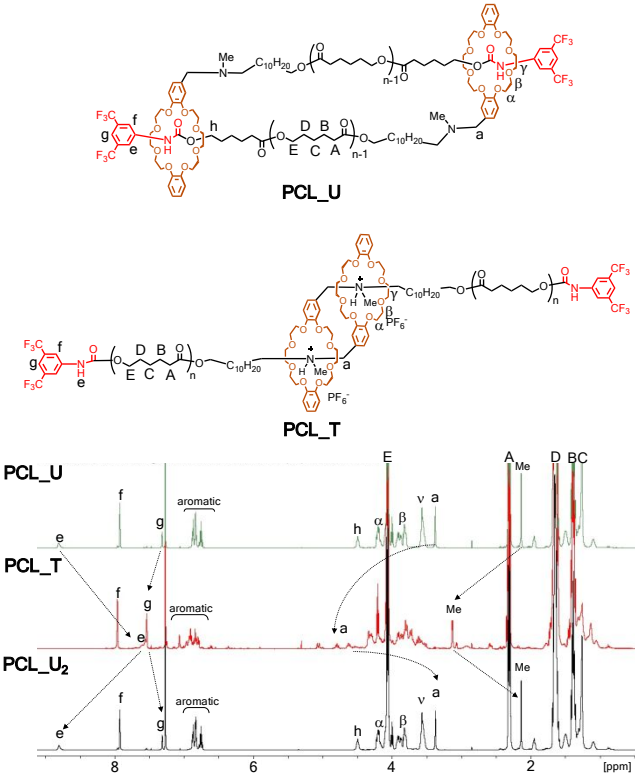

Figure 3. ^{1}H NMR spectra of a) **PCL_U**, b) **PCL_T**, and c) **PCL_U$_2$** (500 MHz, $CDCl_3$, 298 K). The subscript number in **PCL_U$_2$** denotes the number of neutralization/acidification processes.

Cyclic polymers usually display smaller hydrodynamic radii relative to their linear analogues of the same molecular weight. To obtain evidence for the linear-cyclic topology transformation based on the acidification/neutralization-based rotaxane switch, the hydrodynamic volume of the obtained polymers was compared. To avoid unintentional protonation during the GPC measurements on account of the sensitivity of the *tert*-amine group toward acidity, DOSY spectra were recorded to evaluate the change in hydrodynamic volume (Figures 4).

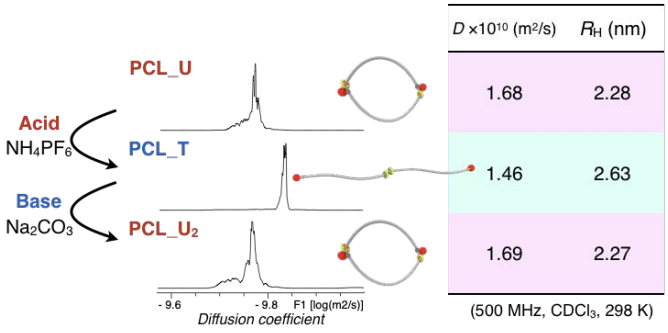

Figure 4. Diffusion constants, D_h, and hydrodynamic radii, R_H, of **PCL_U** (before protonation), **PCL_T** (after protonation), and **PCL_U$_2$** (protonation again) estimated by DOSY spectroscopy. The subscript number in **PCL_U$_2$** denotes the number of neutralization/acidification processes.

Figure 4 shows the obtained diffusion constants, D_h, and hydrodynamic radii, R_H, of **PCL_U** (before protonation) and **PCL_T** (after protonation). For **PCL_U** and **PCL_T**, R_H values of 2.28 nm and 2.63 nm were calculated, respectively. After neutralization of **PCL_T**, the R_H value returned to that of **PCL_U**. The R_H value ratio between **PCL_U** and **PCL_T** (0.87) is in good agreement with previously reported experimental and theoretical data.[30-32] The reversibility of this change in hydrodynamic volume based on the topology changes was confirmed (5 cycles; Figure S6). These results thus corroborate a reversible cyclic-linear topology transformation.

After we demonstrated the reversible cyclic-linear topological transformation in solution ($CHCl_3$), we examined the topologyical effect in the bulk state. For that purpose, we carried out DSC measurements before and after the topology transformation. The results revealed that the glass-transition temperature (T_g) and melting enthalpy of crystalline PCL were reversibly changed upon transforming the topology (Figure 5). The T_g of **PCL_T** was lower (T_g = -52 °C) than that of **PCL_U** (T_g = -46 °C), which is consistent with previously reported topological effects.[33-36] We also noticed a marked difference in the melting behavior of the PCL polymers: The melting peak in **PCL_T** was hardly visible, while **PCL_U** exhibited clear supercooling (around 10 °C) and melting peaks (28-29 °C). The peaks that originate from crystallization of PCL disappeared upon protonation, i.e., upon the topological transform from cyclic to linear. The reversibility of this drastic topology-based change in crystallinity was confirmed (5 cycles; Figure S8).

From the viewpoint of length of polymer chain, the shorter axle polymers hardly form the folded lamellar crystal. It seems to be difficult for **PCL_T** (n = 14 is too short) to form crystal as the linear polymer with rotaxane structure at the center of polymer chain. On the other hand, **PCL_U** form crystal because of cyclic topology, leading to the reversible phase transition based on their topology, i.e., **PCL_T** being an amorphous polymer and **PCL_U** being a crystalline polymer. It should also be noted here that the relatively small molecular mass (DP = 14) of **PCL_U** and **PCL_T** in this study highlighted the topology effect, albeit that further investigations of the impact of the molecular mass are under consideration.

Conclusions

We have developed rotaxane-based cyclic polymers that are synthesized by a combination of automatic quantitative cyclization and reversible topological transformations. A reversible cyclic-linear topological transformation induced by changing the interactions of a crown ether wheel with a protonated *tert*-amine moiety or urethane linkage upon neutralization/acidification of the *tert*-amine moiety, was confirmed by the change of the hydrodynamic volume in solution and the thermal properties in the bulk derived from crystalline poly(ε-caprolactone) (PCL). Because the large-scale synthesis of cyclic polymers can be achieved by utilizing automatic, quantitative, and concentration-independent formation of [c2] daisy chains as the ideal cyclization process and the topological transformation via rotaxane linkage, the combination of the large-scale synthesis of cyclic polymers and the reversible topological transformations which is facilitated by long-range rotaxane switches with simple neutralization/acidification process, would expand the possibility of cyclic polymers as the functional martials. We believe that the system proven here open up new research areas in polymer and materials science.

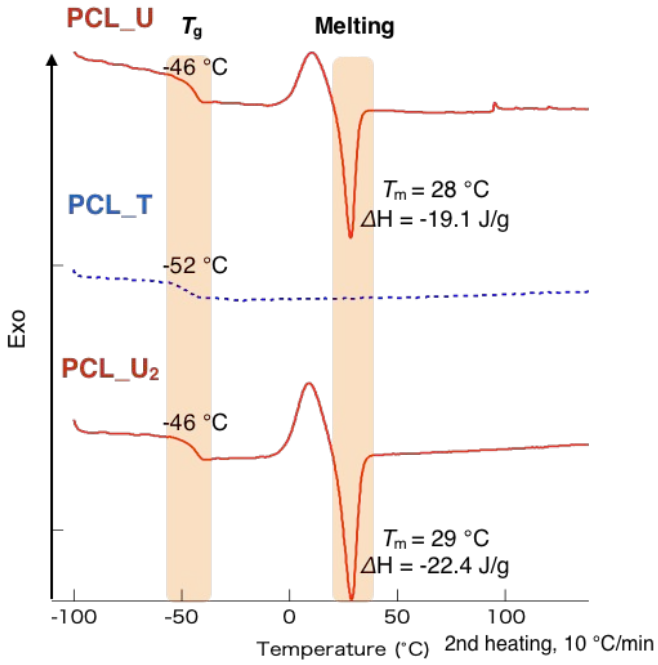

Figure 5. DSC curves of **PCL_U** (before protonation), **PCL_T** (after protonation), and **PCL_U$_2$** (deprotonated again). The subscript number in **PCL_U$_2$** denotes the number of neutralization/acidification processes.

Author Contributions

D. Aoki and G. Aibara contributed equally to this work.

Notes and references

1. Y. Deng, S. Zhang, G. L. Lu and X. Y. Huang, *Polym. Chem.*, 2013, **4**, 1289-1299.
2. B. A. Laurent and S. M. Grayson, *Chem. Soc. Rev.*, 2009, **38**, 2202-2213.
3. S. Honda, T. Yamamoto and Y. Tezuka, *Nat. Commun.*, 2013, **4**, 1574.
4. B. I. Voit and A. Lederer, *Chem. Rev.*, 2009, **109**, 5924-5973.
5. J. E. Poelma, K. Ono, D. Miyajima, T. Aida, K. Satoh and C. J. Hawker, *ACS Nano*, 2012, **6**, 10845-10854.
6. J. H. Lee, P. Driva, N. Hadjichristidis, P. J. Wright, S. P. Rucker and D. J. Lohse, *Macromolecules*, 2009, **42**, 1392-1399.
7. S. Aoshima and S. Kanaoka, *Chem. Rev.*, 2009, **109**, 5245-5287.
8. Z. Guan, P. M. Cotts, E. F. McCord and S. J. McLain, *Science*, 1999, **283**, 2059-2062.
9. F. M. Haque and S. M. Grayson, *Nat. Chem.*, 2020, **12**, 433-444.
10. D. Aoki, *Polym. J.*, 2020, **53**, 257-269.
11. H. Sun, C. P. Kabb, M. B. Sims and B. S. Sumerlin, *Prog. Polym. Sci.*, 2019, **89**, 61-75.
12. O. Altintas, P. Gerstel, N. Dingenouts and C. Barner-Kowollik, *Chem. Commun.* , 2010, **46**, 6291-6293.
13. M. Schappacher and A. Deffieux, *J. Am. Chem. Soc.*, 2011, **133**, 1630-1633.
14. J. Willenbacher, B. V. Schmidt, D. Schulze-Suenninghausen, O. Altintas, B. Luy, G. Delaittre and C. Barner-Kowollik, *Chem. Commun.* , 2014, **50**, 7056-7059.
15. S. Honda, M. Oka, H. Takagi and T. Toyota, *Angew. Chem. Int. Ed.*, 2019, **58**, 144-148.
16. N. Tsurumi, R. Takashima, D. Aoki, S. Kuwata and H. Otsuka, *Angew. Chem. Int. Ed.*, 2020, **59**, 4269-4273.
17. T. Yamamoto, S. Yagyu and Y. Tezuka, *J. Am. Chem. Soc.*, 2016, **138**, 3904-3911.
18. T. Takata, *ACS Cent. Sci.*, 2020, **6**, 129-143.
19. D. Aoki and T. Takata, *Polymer*, 2017, **128**, 276-296.
20. D. Aoki, S. Uchida and T. Takata, *Angew. Chem. Int. Ed.*, 2015, **54**, 6770-6774.
21. H. Sato, D. Aoki and T. Takata, *ACS Macro Lett.*, 2016, **5**, 699-703.
22. D. Aoki, G. Aibara, S. Uchida and T. Takata, *J. Am. Chem. Soc.*, 2017, **139**, 6791-6794.
23. K. Nakazono, T. Ogawa and T. Takata, *Mater. Chem. Front.*, 2019, **3**, 2716-2720.
24. T. Ogawa, K. Nakazono, D. Aoki, S. Uchida and T. Takata, *ACS Macro Lett.*, 2015, **4**, 343-347.
25. T. Ogawa, N. Usuki, K. Nakazono, Y. Koyama and T. Takata, *Chem. Commun.*, 2015, **51**, 5606-5609.
26. S. Valentina, T. Ogawa, K. Nakazono, D. Aoki and T. Takata, *Chem. Eur. J.*, 2016, **22**, 8759-8762.
27. K. Nakazono, S. Kuwata and T. Takata, *Tetrahedron Lett.*, 2008, **49**, 2397-2401.
28. F. Ishiwari, K. Nakazono, Y. Koyama and T. Takata, *Chem. Commun.*, 2011, **47**, 11739-11741.
29. K. Nakazono and T. Takata, *Chem. Eur. J.*, 2010, **16**, 13783-13794.
30. J. N. Hoskins and S. M. Grayson, *Macromolecules*, 2009, **42**, 6406-6413.
31. W. Burchard and M. Schmidt, *Polymer*, 1980, **21**, 745-749.
32. J. A. Castro-Osma, C. Alonso-Moreno, J. C. Garcia-Martinez, J. Fernandez-Baeza, L. F. Sanchez-Barba, A. Lara-Sanchez and A. Otero, *Macromolecules*, 2013, **46**, 6388-6394.
33. M. E. Córdova, A. T. Lorenzo, A. J. Müller, J. N. Hoskins and S. M. Grayson, *Macromolecules*, 2011, **44**, 1742-1746.
34. H. H. Su, H. L. Chen, A. Diaz, M. T. Casas, J. Puiggali, J. N. Hoskins, S. M. Grayson, R. A. Perez and A. J. Muller, *Polymer*, 2013, **54**, 846-859.
35. R. A. Perez, M. E. Cordova, J. V. Lopez, J. N. Hoskins, B. Zhang, S. M. Grayson and A. J. Muller, *React. Funct. Polym.*, 2014, **80**, 71-82.
36. Z. L. Li, J. Wang, R. A. Perez-Camargo, A. J. Muller, B. Y. Zhang, S. M. Grayson and W. B. Hu, *Polym. Int.*, 2016, **65**, 1074-1079.